JOURNAL OF GUIDANCE, CONTROL, AND DYNAMICS
Vol. 20, No. 6, November–December 1997

Nonlinear Control of a Prototypical Wing Section with Torsional Nonlinearity

Jeonghwan Ko,* Andrew J. Kurdila,† and Thomas W. Strganac‡
Texas A&M University, College Station, Texas 77843-3141

With the increase in popularity of active materials for control actuation, renewed interest is evident in the derivation of control methodologies for aeroelastic systems. It has been known for some time that prototypical aeroelastic wing sections can exhibit a broad class of pathological response regimes when the system includes certain types of nonlinearities. We investigate nonlinear control laws for aeroelastic systems that include polynomial structural nonlinearities and study the closed-loop stability of the system. It is shown that locally asymptotically stable (nonlinear) feedback controllers can be derived for the aeroelastic system using partial feedback linearization techniques. In this case, the stability results are necessarily local in nature and are derived by considering stability of the associated zero dynamics subsystem. It is also demonstrated that globally stable (nonlinear) adaptive control methods can be derived for a class of aeroelastic systems under consideration. Numerical simulations are used to provide empirical validation of some of the results.

Nomenclature

a	= nondimensionalized distance from the midchord to the elastic axis
b	= semichord of the wing
c_h	= structural damping coefficient in plunge due to viscous damping
c_α	= structural damping coefficient in pitch due to viscous damping
h	= plunge displacement
I_α	= mass moment of inertia of the wing about the elastic axis
k_h	= structural spring constant in plunge
k_α	= structural spring constant in pitch
m	= mass
U	= freestream velocity
x_α	= nondimensionalized distance measured from the elastic axis to the center of mass
α	= pitch angle
β, β_1, β_2	= flap deflection
ρ	= density of air

I. Introduction

ACTIVE control of aeroelastic response is examined and, in particular, appropriate control strategies for nonlinear aeroelastic systems are addressed in this paper. Aeroelasticity is the interaction of structural, inertial, and aerodynamic forces. Flutter is an oscillatory aeroelastic instability characterized by the loss of system damping due to the presence of unsteady aerodynamic loads.[1] Theodorsen[2] developed the classical unsteady aerodynamic theory that accounts for the aerodynamic (lag) damping at different flow conditions and frequencies. Theodorsen and Garrick[3] predict flutter velocities and frequencies and compare these predictions of flutter with experimental results. Wagner and Jones (see Ref. 1) develop approximations of Theodorsen's function that are appropriate to simulate wing motion and predict aeroelastic response in unsteady aerodynamic flow.

Using the developments by Wagner and Jones, several researchers have attempted to further understand the control of unsteady motion of an airfoil. Lyons et al.[4] used a method of converting the Jones approximation into the Laplace domain and augmenting the states of the system to account for the lag terms in the aerodynamics. This approach structured the equations of motion for control law development. Vepa[5] developed a Padé approximation technique to describe both Wagner's function and Theodorsen's function in the frequency domain. Edwards et al.[6] compared the methods of Lyons et al.[4] and Vepa.[5] Furthermore, Edwards et al.[6] examined these developments by dividing the circulatory terms of the lift into rational and nonrational portions inasmuch as the nonrational part could not be written as a ratio of polynomials. Edwards et al.'s approach reduced the number of augmented states previously required to model the unsteady aerodynamics. These methods are developed for arbitrary, but small, motion of a wing.

Many strategies have been examined to control unacceptable wing response or suppress flutter. Lyons et al.[4] investigated full-state feedback with a Kalman estimator for the purpose of flutter suppression. The theoretical model was relatively simple and required only eight states. Mukhopadhyay et al.[7] and Gangsaas et al.[8] created 20th- and 50th-order models, respectively. They developed methods to reduce these higher-order systems to show the practicality of these control strategies. These control systems implemented estimators to describe unmeasured states and used estimated state feedback as the control method. Karpel[9] compared the aerodynamic descriptions of Lyons et al.,[4] Vepa,[5] and Edwards et al.[6] to develop partial-state feedback controllers. Karpel[9] used pole placement techniques to develop the control laws for flutter suppression and gust alleviation.

Horikawa and Dowell[10] performed flutter analysis with control, employing proportional gain feedback methods developed from root locus plots. They used a quasisteady aerodynamic model coupled with a two-degree-of-freedom structural model to develop several types of feedback. The development directly feeds one of four variables to the control surface through a proportional gain. Heeg[11] investigated flutter suppression by control with piezoelectric actuators and increased the flutter velocity by 20%. The work involved a small wing model mounted on spring tines to simulate the bending and torsion modes. Four actuators were mounted to control the bending mode. Heeg's[11] analysis employs a classic approach for control, by using root locus plots to derive proportional gain feedback control laws.

Lin,[12] Lazarus,[13] and Lazarus et al.[14] analyzed a typical section model. The study included control of the bending and torsion modes by piezoelectric actuators mounted on the wing and additional

Received Nov. 10, 1996; presented as Paper 97-0580 at the AIAA 35th Aerospace Sciences Meeting, Reno, NV, Jan. 6–9, 1997; revision received April 14, 1997; accepted for publication April 18, 1997.

*Postdoctoral Research Associate, Department of Aerospace Engineering. Member AIAA.

†Associate Professor, Department of Aerospace Engineering. Member AIAA.

‡Associate Professor, Department of Aerospace Engineering. Associate Fellow AIAA.

control with leading- and trailing-edge flaps. This structure and control scheme was designed for wind-tunnel disturbance rejection, gust alleviation, and flutter suppression. They showed that direct control through piezoelectrics was possible. Their design strategy used full-state feedback with an estimator. Lazarus[13] performed a more complete experimental analysis to validate the results of the typical section model.

These researchers have shown that linear theory can be applicable for control of aeroelastic systems. Unfortunately, as aircraft performance increases, so does the needs for more sophisticated aeroelastic models. Aeroelastic systems typically contain nonlinearities, which are either neglected or simplified to a linear form for analysis. Nonlinearities that occur in aeroelastic systems include control saturation, free play, hysteresis, piecewise linear, and continuous nonlinearities. Control saturation occurs when an increasing input into a control actuator will no longer increase the output of the system. This nonlinearity occurs in most motor controllers when their operational limits are exceeded. Free play is seen in control surface linkages or hinges in which the surface will not move until the magnitude of the input exceeds a certain value. Hysteresis occurs in systems in which friction affects linkage dynamics or in which rivet connections slip on a wing. A nonlinear stiffness may be observed in the large bending of wings and rotor blades or in control actuators that become increasingly harder to deflect as they are moved farther from the neutral position. Many researchers have examined the nonlinearities inherent in structural models.

Woolston et al.[15] investigated nonlinearities in structural stiffness and control surface linkages. They created a model with free play, hysteresis, cubic-hardening, and cubic-softening nonlinearities in the torsional mode. For general wing motion, they observed that the flutter velocity lowered as the initial disturbance grew and that the stability of the system was highly dependent on the magnitude of the initial condition. A cubic-softening spring stiffness lowered the flutter velocity. They also noted that cubic hardening caused limit cycle oscillations rather than flutter at velocities above the open-loop flutter velocity.

Breitbach[16] showed that a poor agreement between theory and experiment in flutter is most likely due to nonlinear structural stiffness in models. He also presented a detailed examination of many types of nonlinearities that may affect aeroelastic systems. Tang and Dowell[17] introduced a free play nonlinearity in the torsional stiffness and examined the nonlinear aeroelastic response. For various initial conditions, they created maps of the system response to describe locations of periodic limit cycles, chaotic motion, and divergent motion. They concluded that limit cycle motion is dependent on freestream velocity, initial pitch condition, magnitude of the free play nonlinearity, and initial conditions.

Lee and LeBlanc[18] performed analysis of a nonlinear wing model using a time-marching scheme that simulated aeroelastic response. Models of softening and hardening cubic springs were examined by varying the mass ratio, by increasing the distance between the elastic axis and the center of mass, and by varying the ratio of the plunge frequency to pitch frequency. For the softening spring case, unstable motion was encountered below the linear flutter speed for nearly every parameter; increasing the nonlinearity and increasing the mass ratio tended to make the system more unstable at lower velocities. For the hardening spring case, limit cycle oscillations were always present instead of divergent flutter. Varying the parameters of the hardening spring case affected the amplitudes of the limit cycles.

These researchers have developed models for exploring nonlinear aeroelasticity and have also attempted to describe the motion with time marching solutions and describing function analysis. However, efforts to examine nonlinear aeroelasticity and active control strategies are limited. O'Neil and Strganac[19,20] and O'Neil et al.[21] examine nonlinear aeroelastic response via a unique experimental apparatus that permits a prescribed linear or nonlinear structural stiffness. With nonlinear structural stiffness, the model exhibits limit cycle oscillations. Various full-state feedback control laws have been examined with the aeroelastic model with a control surface.[22] An unsteady aerodynamic model is developed with an approximation to Theodorsen's function, and a Kalman estimator is used to estimate the augmented state system. Tests of the linear structural model and nonlinearities are examined while the performance of the control is verified for numerous flow conditions using the linear controller. In many flow regimes, the linear control design was highly effective. Roughly speaking, control of the nonlinear system during limit cycle oscillations was ineffective, unpredictable, or poorly understood.

Whereas several authors have investigated the effectiveness of linear and adaptive control methodologies for aeroelastic systems, our own experimental investigations have provided experimental evidence that linear control methods may not be reliable when nonlinear effects predominate.[22] In addition, it is typically the case that even fewer analytical results are available that guarantee the closed-loop stability of nonlinear adaptive control methods. Thus, we seek to derive nonlinear control methodologies that make as much use of the knowledge of the nonlinearities as possible. In all of our analyses, a primary goal is to make definitive statements regarding the closed-loop stability of the system. Our strategy has been to simplify the model and incorporate the essential and well-understood structural nonlinearities as a precursor to methods that accommodate more complex nonlinearities associated with aerodynamics. Dead-zone, hysteretic, and polynomial nonlinearities in the structural system have been investigated in Refs. 17 and 23–25. However, in comparison to the nonlinearities and uncertainties in the aerodynamic component of the dynamical system, the structural nonlinearities are well characterized. To derive a controller that accounts for some of the nonlinearities in the system, we retain the nonlinear torsional stiffness terms. This dynamical system is the simplest possible model that remains a faithful representation of the physics we seek to address, i.e., limit cycle oscillations. If the structurally nonlinear terms are neglected, limit cycle oscillations in our model near the critical velocity are not observed. Certainly, we can add additional nonlinear terms, particularly those that model aerodynamic effects, but the structurally nonlinear terms constitute the bare minimum required to represent limit cycle oscillations at low speeds.

The remainder of this paper discusses two control designs based on partial feedback linearization techniques. In the first case, we derive a nonlinear controller that guarantees the exponential stability of the pitch dynamics subsystem. However, because the system is not fully feedback linearizable, decreasing pitch oscillations inject energy into the associated, remaining reduced degrees of freedom. Still, local asymptotic stability for the closed-loop system can be established by considering the zero dynamics of the system. The local asymptotic closed-loop stability of this pitch primary control depends parametrically on the flow velocity and elastic axis location. A similar control methodology is derived in the second part of the paper for the plunge dynamics subsystem. Finally, we close by showing that, for a very simple but structurally nonlinear aeroelastic model with two control surfaces, the dynamical system is exactly feedback linearizable and global stability results can be derived.

II. Equations of Motion

We consider the problem of flutter suppression for the prototypical aeroelastic wing sections, as shown in Fig. 1. This type of model has been traditional for the experimental and theoretical analyses of two-dimensional aeroelastic behavior. The unique features of the model considered herein are variable location of the elastic axis and the capability of incorporating various types of stiffness for the pitch axis motion. Obviously, the two parameters, elastic axis location and freestream velocity, play critical roles in system stability. A significant portion of this paper will study their importance in some closed-loop control systems. As shown in Refs. 19–21, the governing equations of motion for the aeroelastic model are derived to be

$$\begin{bmatrix} m & mx_\alpha b \\ mx_\alpha b & I_\alpha \end{bmatrix} \begin{Bmatrix} \ddot{h} \\ \ddot{\alpha} \end{Bmatrix} + \begin{bmatrix} c_h & 0 \\ 0 & c_\alpha \end{bmatrix} \begin{Bmatrix} \dot{h} \\ \dot{\alpha} \end{Bmatrix} + \begin{bmatrix} k_h & 0 \\ 0 & k_\alpha(\alpha) \end{bmatrix} \begin{Bmatrix} h \\ \alpha \end{Bmatrix} = \begin{Bmatrix} -L \\ M \end{Bmatrix} \tag{1}$$

where h represents the plunge motion. In these equations, m is the mass of the wing; c_α and c_h are pitch and plunge structural damping coefficients, respectively; and L and M are the aerodynamic lift

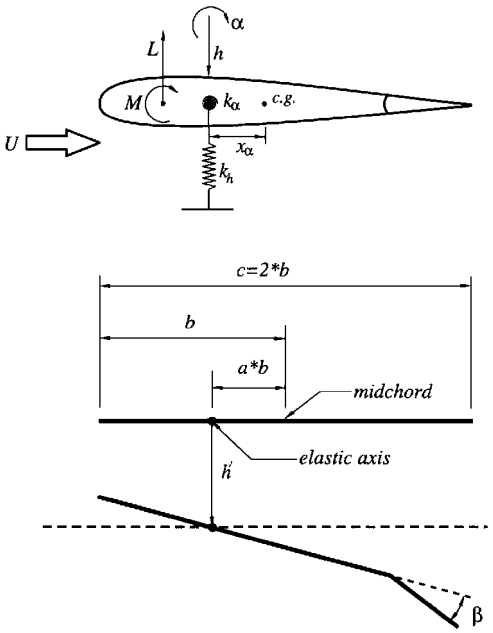

Fig. 1 Aeroelastic model.

and moment. We assume the quasisteady aerodynamic forces and moments are modeled as follows[1]:

$$L = \rho U^2 b c_{l_\alpha}\left[\alpha + (\dot{h}/U) + \left(\tfrac{1}{2} - a\right)b(\dot{\alpha}/U)\right] + \rho U^2 b c_{l_\beta}\beta$$
$$M = \rho U^2 b^2 c_{m_\alpha}\left[\alpha + (\dot{h}/U) + \left(\tfrac{1}{2} - a\right)b(\dot{\alpha}/U)\right] + \rho U^2 b^2 c_{m_\beta}\beta \tag{2}$$

where c_{l_α} and c_{m_α} are lift and moment coefficients per angle of attack and c_{l_β} and c_{m_β} are lift and moment coefficient per control surface deflection. Several classes of nonlinear stiffness contributions $k_\alpha(\alpha)$ have been studied in papers treating the open-loop dynamics of aeroelastic systems (see, for example, Refs. 17 and 23–25). For purposes of illustration, polynomial nonlinearities are introduced at this point. For example, the polynomial nonlinearities might be expressed as

$$k_\alpha(\alpha) = k_{\alpha_0} + k_{\alpha_1}\alpha + k_{\alpha_2}\alpha^2 + k_{\alpha_3}\alpha^3 + k_{\alpha_4}\alpha^4 + \cdots \tag{3}$$

Combining the two equations [Eqs. (1) and (2)], we obtain the equations of motion as

$$\begin{bmatrix} m & mx_\alpha b \\ mx_\alpha b & I_\alpha \end{bmatrix}\begin{Bmatrix} \ddot{h} \\ \ddot{\alpha} \end{Bmatrix} + \begin{bmatrix} c_h + \rho U b c_{l_\alpha} & \rho U b^2 c_{l_\alpha}\left(\frac{1}{2} - a\right) \\ \rho U b^2 c_{m_\alpha} & c_\alpha - \rho U b^3 c_{m_\alpha}\left(\frac{1}{2} - a\right) \end{bmatrix}\begin{Bmatrix} \dot{h} \\ \dot{\alpha} \end{Bmatrix} + \begin{bmatrix} k_h & \rho U^2 b c_{l_\alpha} \\ 0 & -\rho U^2 b^2 c_{m_\alpha} + k_\alpha(\alpha) \end{bmatrix}\begin{Bmatrix} h \\ \alpha \end{Bmatrix} = \begin{Bmatrix} -\rho b c_{l_\beta} \\ \rho b^2 c_{m_\beta} \end{Bmatrix} U^2\beta$$

For the analysis to follow, it is useful to convert this equation into a state-space formulation. We define the state variable as

$$\boldsymbol{x} = \begin{Bmatrix} x_1 \\ x_2 \\ x_3 \\ x_4 \end{Bmatrix} = \begin{Bmatrix} h \\ \alpha \\ \dot{h} \\ \dot{\alpha} \end{Bmatrix}$$

The transformed equations of motion become

$$\dot{\boldsymbol{x}} = \boldsymbol{f}_\mu(\boldsymbol{x}) + \boldsymbol{g}(\boldsymbol{x})U^2\beta \tag{4}$$

Table 1 System variables

$d = m\left(I_\alpha - mx_\alpha^2 b^2\right)$
$k_1 = I_\alpha k_h/d, \qquad k_2 = \left(I_\alpha \rho b c_{l_\alpha} + mx_\alpha b^3 \rho c_{m_\alpha}\right)/d$
$k_3 = -mx_\alpha b k_h/d, \qquad k_4 = \left(-mx_\alpha b^2 \rho c_{l_\alpha} - m\rho b^2 c_{m_\alpha}\right)/d$
$p(x_2) = (-mx_\alpha b/d)k_\alpha(x_2), \qquad q(x_2) = (m/d)k_\alpha(x_2)$
$c_1 = \left[I_\alpha\left(c_h + \rho U b c_{l_\alpha}\right) + mx_\alpha \rho U b^3 c_{m_\alpha}\right]/d$
$c_2 = \left[I_\alpha \rho U b^2 c_{l_\alpha}\left(\frac{1}{2} - a\right) - mx_\alpha b c_\alpha + mx_\alpha \rho U b^4 c_{m_\alpha}\left(\frac{1}{2} - a\right)\right]/d$
$c_3 = \left(-mx_\alpha b c_h - mx_\alpha \rho U b^2 c_{l_\alpha} - m\rho U b^2 c_{m_\alpha}\right)/d$
$c_4 = \left[mc_\alpha - mx_\alpha \rho U b^3 c_{l_\alpha}\left(\frac{1}{2} - a\right) - m\rho U b^3 c_{m_\alpha}\left(\frac{1}{2} - a\right)\right]/d$
$g_3 = (1/d)\left(-I_\alpha \rho b c_{l_\beta} - mx_\alpha b^3 \rho c_{m_\beta}\right)$
$g_4 = (1/d)\left(mx_\alpha b^2 \rho c_{l_\beta} + m\rho b^2 c_{m_\beta}\right)$

Table 2 System parameters

Property	Value
b	0.135 m
span	0.6 m
k_h	2844.4 N/m
c_h	27.43 Ns/m
c_α	0.036 Ns
ρ	1.225 kg/m^3
c_{l_α}	6.28
c_{l_β}	3.358
c_{m_α}	$(0.5 + a)c_{l_\alpha}$
c_{m_β}	−0.635

where

$$\boldsymbol{f}_\mu = \begin{Bmatrix} x_3 \\ x_4 \\ -k_1 x_1 - \left[k_2 U^2 + p(x_2)\right]x_2 - c_1 x_3 - c_2 x_4 \\ -k_3 x_1 - \left[k_4 U^2 + q(x_2)\right]x_2 - c_3 x_3 - c_4 x_4 \end{Bmatrix}$$

$$\boldsymbol{g}(\boldsymbol{x}) = \begin{Bmatrix} 0 \\ 0 \\ g_3 \\ g_4 \end{Bmatrix}$$

To simplify their form, several auxiliary variables are introduced (as shown in Table 1). Note that the equations of motion are dependent on the freestream velocity U and also on the elastic axis location a. The notation $\boldsymbol{f}_\mu(\boldsymbol{x})$ is conventional in that it emphasizes the parametric dependence of the dynamics on U and a. Strictly speaking, the subscript μ should be replaced by the vector of the parameters $\{U, a\}$. We adopt the simpler notation, keeping in mind that the solutions are in fact a two-parameter family of solutions.

III. Open-Loop Equations/Limit Cycles

It is well known that the equations of motion just derived exhibit limit cycle oscillations (LCO), as well as other nonlinear response regimes including chaotic response.[19,23,25] The system parameters to be used in the following numerical investigations are given in Table 2. These data are obtained from the experimental model described in full detail in Refs. 19–21. The nonlinear stiffness term $k_\alpha(\alpha)$ is obtained by curve fitting the measured displacement–moment data for a nonlinear spring as[19]

$$k_\alpha(\alpha) = 2.82(1 - 22.1\alpha + 1315.5\alpha^2 - 8580\alpha^3 + 17{,}289.7\alpha^4) \tag{5}$$

With the flow velocity $U = 15$ m/s and the initial conditions of $\alpha = 0.1$ rad and $y = 0.01$ m, the resulting time response of the nonlinear system is shown in Figs. 2 and 3. Clearly the system exhibits LCO behavior and is in good qualitative agreement with the behavior expected in this class of systems. The relations between

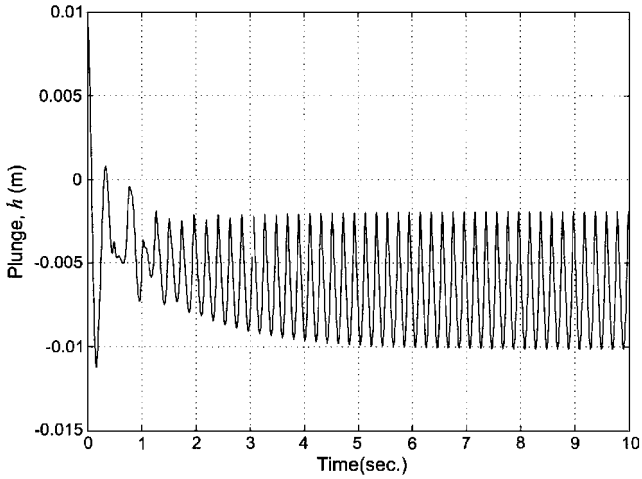

Fig. 2 Open-loop response: plunge.

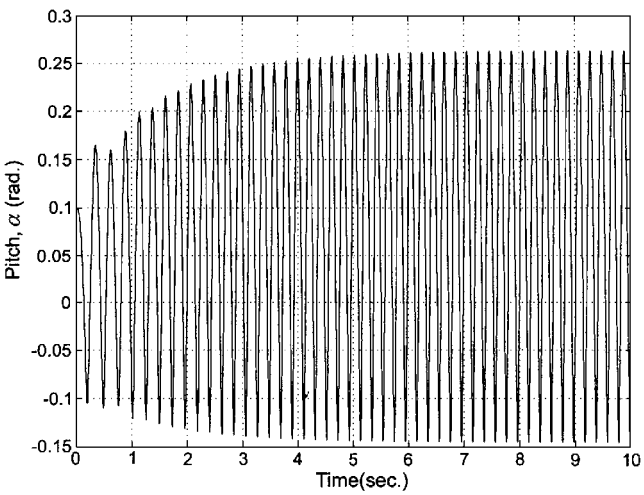

Fig. 3 Open-loop response: pitch.

LCO frequencies, magnitudes, and initial conditions or flow velocities are shown in Refs. 19–21. There have been some efforts to control the system using a linear controller.[22] As one might easily expect, however, a linear controller cannot effectively stabilize a system that undergoes severe nonlinear motions, and there is a need to design a controller based on nonlinear control methodologies.

IV. Feedback Linearization

We utilize the method of partial feedback linearization to derive viable control methodologies for the nonlinear aeroelastic system. A detailed description of the feedback linearization methods is beyond the scope of this paper and can be found in various texts, e.g., Refs. 26 and 27. Roughly speaking, the method consists of constructing a coordinate transformation, which transforms the system equation to a companion form and selects a nonlinear feedback control law to cancel the nonlinear dynamics. In the most fortunate circumstances, the resulting system is a linear equivalent model, to which modern linear control theory can be easily applied.

However, a given nonlinear system is not always fully linearizable. Depending on the relative degree of the nonlinear system of concern, the nonlinear transformation results in either a partially or a fully linearized equivalent system. The relative degree of an output function is defined to be the number of differentiation of output $y(\boldsymbol{x})$ to have the input u appear explicitly.[27] This definition of the relative degree is an extension of the one for linear systems: the number of excessive poles over the number of zeros. For the case when the system is partially linearized, there exists a hidden internal dynamics whose stability must be investigated to ensure the stability of the whole system.[27] Because it is difficult to find an output function $y(\boldsymbol{x})$ that yields complete feedback linearization for the two outputs (h, α) in the aeroelastic system with one control surface, we begin by studying two separate problems in which we consider one output variable at a time.

A. Pitch Primary Control

In our first study, we will show that the nonlinear equations can be stabilized (at least locally) using partial feedback linearization based on the pitch angle. Because the output and feedback variable are selected to be the pitch angle, we denote this method as pitch primary control. We begin by calculating the relative degree associated with the following output variable:

$$y(\boldsymbol{x}) = x_2 (= \alpha) \tag{6}$$

That is, the objective of the control is to stabilize the pitch output α. The relative degree of this output is calculated as follows[26]:

$$y(\boldsymbol{x}) = x_2, \qquad L_g y(\boldsymbol{x}) = 0$$

$$L_f y(\boldsymbol{x}) = x_4, \qquad L_g L_f y(\boldsymbol{x}) = g_4 \neq 0$$

where $L_f y(\boldsymbol{x})$ is a Lie derivative of y in the direction of $\boldsymbol{f}$ defined as[26,27]

$$L_f y(\boldsymbol{x}) = \sum_i \frac{\partial y}{\partial x_i} \cdot f_i, \qquad L_g L_f y(\boldsymbol{x}) = L_g [L_f y(\boldsymbol{x})] \tag{7}$$

Thus, we have confirmed that the relative degree of the system is $r = 2$. In other words, two degrees of freedom of the system can be linearized. To accomplish partial feedback linearization, we consider the following state transformation:

$$\boldsymbol{x} \mapsto \boldsymbol{\phi}$$

$$\phi_1 = y(\boldsymbol{x}) = x_2, \qquad \phi_2 = L_f y(\boldsymbol{x}) = x_4 \tag{8}$$

$$\phi_3 = x_1, \qquad \phi_4 = -g_3 x_4 + g_4 x_3$$

which just happens to be linear. Carefully note that the transforms for ϕ_3 and ϕ_4 are defined such that $L_g \phi_3$ and $L_g \phi_4 = 0$.

To validate that the preceding transformation is admissible, we need to check the invertibility of the Jacobian of the mapping. The coordinate transformation just defined is

$$\begin{Bmatrix} \phi_1 \\ \phi_2 \\ \phi_3 \\ \phi_4 \end{Bmatrix} = \begin{Bmatrix} x_2 \\ x_4 \\ x_1 \\ -g_3 x_4 + g_4 x_3 \end{Bmatrix}$$

$$\begin{Bmatrix} x_1 \\ x_2 \\ x_3 \\ x_4 \end{Bmatrix} = \begin{Bmatrix} \phi_3 \\ \phi_1 \\ (1/g_4)(\phi_4 + g_3 \phi_2) \\ \phi_2 \end{Bmatrix} \tag{9}$$

The Jacobian matrices of the transform and the inverse transform are

$$\left[\frac{\partial \phi_i}{\partial x_j}\right] = \begin{bmatrix} 0 & 1 & 0 & 0 \\ 0 & 0 & 0 & 1 \\ 1 & 0 & 0 & 0 \\ 0 & 0 & g_4 & -g_3 \end{bmatrix}$$

$$\left[\frac{\partial x_i}{\partial \phi_j}\right] = \begin{bmatrix} 0 & 0 & 1 & 0 \\ 1 & 0 & 0 & 0 \\ 0 & g_3/g_4 & 0 & 1/g_4 \\ 0 & 1 & 0 & 0 \end{bmatrix} \tag{10}$$

Inasmuch as both Jacobians have nonzero determinants, clearly the transform is well defined. With the preceding transformation, the governing equations of motion for the system become

$$\begin{Bmatrix}\dot{\phi}_1\\ \dot{\phi}_2\\ \dot{\phi}_3\\ \dot{\phi}_4\end{Bmatrix} = \begin{Bmatrix}\phi_2\\ -P_U(\phi_1)\phi_1 - [c_4 + c_3(g_3/g_4)]\phi_2 - k_3\phi_3 - (c_3/g_4)\phi_4\\ (g_3/g_4)\phi_2 + (1/g_4)\phi_4\\ [g_3P_U(\phi_1) - g_4Q_U(\phi_1)]\phi_1 + \left[-c_1g_3 - c_2g_4 + c_3\left(g_3^2/g_4\right) + c_4g_3\right]\phi_2\\ \quad + (k_3g_3 - k_1g_4)\phi_3 + [c_3(g_3/g_4) - c_1]\phi_4\end{Bmatrix} + \begin{Bmatrix}0\\ g_4\\ 0\\ 0\end{Bmatrix} U^2\beta \tag{11}$$

where

$$P_U(\phi_1) = k_4U^2 + q(\phi_1), \qquad Q_U(\phi_1) = k_2U^2 + p(\phi_1) \tag{12}$$

Now, partial feedback linearization can be achieved by setting the control input β to be

$$\beta = \frac{P_U(\phi_1)\phi_1 + [c_4 + c_3(g_3/g_4)]\phi_2 + k_3\phi_3 + (c_3/g_4)\phi_4 + v}{U^2g_4} \tag{13}$$

where v is a new, yet to be defined, control. The resulting partially linearized equations are

$$\dot{\phi}_1 = \phi_2, \qquad \dot{\phi}_2 = v, \qquad \dot{\phi}_3 = A_{32}\phi_2 + A_{34}\phi_4$$
$$\dot{\phi}_4 = [g_3P_U(\phi_1) - g_4Q_U(\phi_1)]\phi_1 + A_{42}\phi_2 + A_{43}\phi_3 + A_{44}\phi_4 \tag{14}$$

where

$$A_{32} = g_3/g_4, \qquad A_{34} = 1/g_4$$
$$A_{42} = -c_1g_3 - c_2g_4 + c_3\left(g_3^2/g_4\right) + c_4g_3$$
$$A_{43} = k_3g_3 - k_1g_4, \qquad A_{44} = (c_3g_3/g_4) - c_1$$

By judiciously choosing v, we make the linearized dynamics for ϕ_1 and ϕ_2 exponentially stable. We can use any linear control design technique for the linear subsystem $\{\phi_1, \phi_2\}$. However, the subsystem $\{\phi_3, \phi_4\}$ is not affected directly by the new input v and we do not have direct control over this subsystem. Note that the internal dynamics for ϕ_3 and ϕ_4 are still nonlinear. Generally, it is not easy to investigate the stability of the internal dynamics.[27] However, by checking the stability of the zero dynamics of the partially linearized system, we can obtain stability information on the internal dynamics. Let $\phi_1 = 0$; then clearly $\phi_2 = 0$ and the equation of internal dynamics is

$$\begin{Bmatrix}\dot{\phi}_3\\ \dot{\phi}_4\end{Bmatrix} = \begin{bmatrix}0 & A_{34}\\ A_{43} & A_{44}\end{bmatrix}\begin{Bmatrix}\phi_3\\ \phi_4\end{Bmatrix} \tag{15}$$

We observe the zero dynamics is linear and the stability of these zero dynamics will ensure the stability of the entire system, at least locally. The eigenvalues of the zero dynamics are

$$\lambda = \frac{A_{44} \pm \sqrt{A_{44}^2 + 4A_{34}A_{43}}}{2} \tag{16}$$

Note that the stability of the zero dynamics depends on the flow velocity U and on the elastic axis location a, although it is not explicitly shown. With the quantities defined in Table 1, the real parts of the eigenvalues of the zero dynamics are plotted with respect to a in Fig. 4 ($U = 15$ m/s). Observe that for $a > -0.55$ the real parts of both eigenvalues are negative and, thus, the zero dynamics is stable. With $a = -0.4$ and $U = 15$ m/s and with the initial conditions $\alpha = 0.1$ rad and $y = 0.01$ m, the time response of the system is shown in Fig. 5. We have chosen the modified input $v = -1.2\dot{\alpha} - 4\alpha$ such that the closed subsystem has poles at $s = -0.6 \pm 1.9079$. It should be emphasized, however, that the stability of the zero dynamics only guarantees the local stability of the internal dynamics.

B. Plunge Primary Control

In this section we show that the nonlinear equations can be stabilized (at least locally) using partial feedback linearization in terms of the plunge variable. As in the preceding case, we denote this analysis as the plunge primary control. We begin by investigating the relative degree with the following output variable:

$$y(\boldsymbol{x}) = x_1(= h) \tag{17}$$

That is, the objective of the control is to stabilize the plunge output h. The relative degree of the preceding output is calculated as follows:

$$y(\boldsymbol{x}) = x_1, \qquad L_gy(\boldsymbol{x}) = 0$$
$$L_fy(\boldsymbol{x}) = x_3, \qquad L_gL_fy(\boldsymbol{x}) = g_3 \neq 0$$

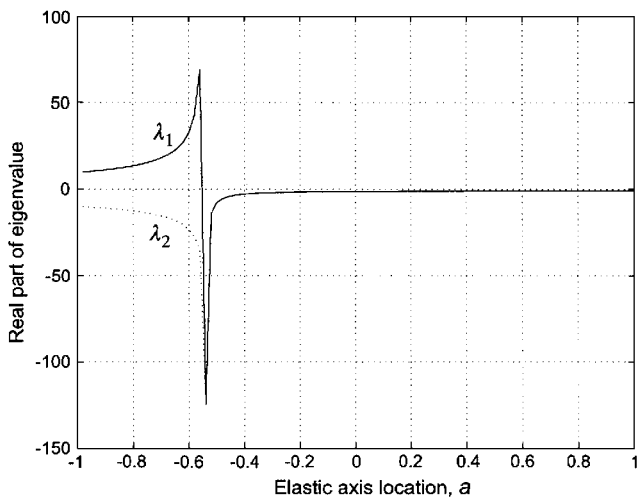

Fig. 4 Real parts of eigenvalues of zero dynamics with respect to a: pitch primary, $U = 15$ m/s.

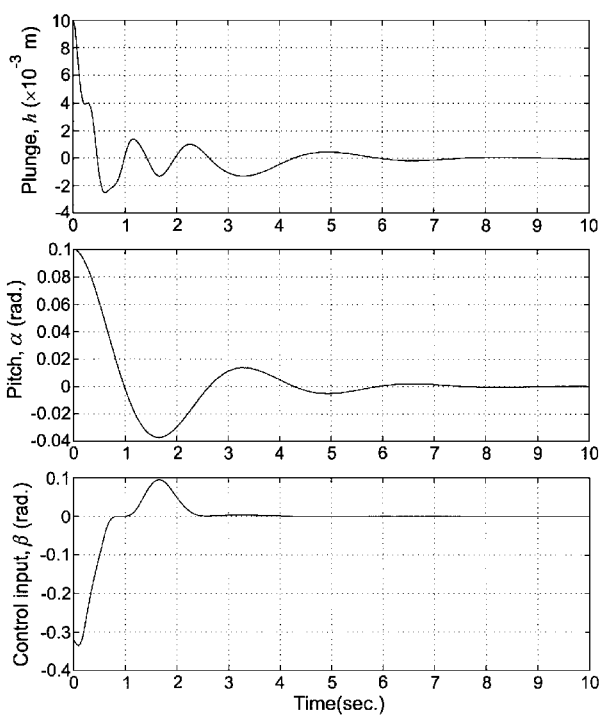

Fig. 5 Time response of pitch primary control: $a = -0.4$ and $U = 15$ m/s.

We have consequently confirmed that the relative degree of the system is $r = 2$. The state transformation we choose for the current case is

$$\boldsymbol{x} \mapsto \boldsymbol{\phi}$$

$$\phi_1 = y(\boldsymbol{x}) = x_1, \qquad \phi_2 = L_f y(\boldsymbol{x}) = x_3 \tag{18}$$

$$\phi_3 = x_2, \qquad \phi_4 = g_3 x_4 - g_4 x_3$$

Again, the transforms for ϕ_3 and ϕ_4 are defined such that $L_g\phi_3$ and $L_g\phi_4 = 0$. The preceding transform is well defined due to the nonsingularity of the Jacobian as before. The governing equations of the system become

$$\begin{Bmatrix} \dot{\phi}_1 \\ \dot{\phi}_2 \\ \dot{\phi}_3 \\ \dot{\phi}_4 \end{Bmatrix} = \begin{Bmatrix} \phi_1 \\ -k_1\phi_1 - [c_1 + c_2(g_4/g_3)]\phi_2 - Q_U(\phi_3)\phi_3 - (c_2/g_3)\phi_4 \\ (g_4/g_3)\phi_2 + (1/g_3)\phi_4 \\ (g_4k_1 - g_3k_3)\phi_1 + \left[c_1g_4 + c_2\left(g_4^2/g_3\right) - c_3g_3 - c_4g_4\right]\phi_2 \\ \quad + [g_4Q_U(\phi_3) - g_3P_U(\phi_3)]\phi_3 + [c_2(g_4/g_3) - c_4]\phi_4 \end{Bmatrix} + \begin{Bmatrix} 0 \\ g_3 \\ 0 \\ 0 \end{Bmatrix} \mu\beta \tag{19}$$

where

$$P_U(\phi_3) = k_4U^2 + q(\phi_3), \qquad Q_U(\phi_3) = k_2U^2 + p(\phi_3) \tag{20}$$

Clearly, from Eq. (19), the feedback linearization can be achieved by setting the control input β to be

$$\beta = \frac{k_1\phi_1 + [c_1 + c_2(g_4/g_3)]\phi_2 + Q_U(\phi_3)\phi_3 + (c_2/g_3)\phi_4 + v}{U^2 g_3} \tag{21}$$

The resulting partially linearized equation is

$$\dot{\phi}_1 = \phi_2, \qquad \dot{\phi}_2 = v, \qquad \dot{\phi}_3 = A_{32}\phi_2 + A_{34}\phi_4$$
$$\dot{\phi}_4 = A_{41}\phi_1 + A_{42}\phi_2 + [g_4Q_U(\phi_3) - g_3P_U(\phi_3)]\phi_3 + A_{44}\phi_4 \tag{22}$$

where

$$A_{32} = g_4/g_3, \qquad A_{34} = 1/g_3, \qquad A_{41} = g_4k_1 - g_3k_3$$
$$A_{42} = c_1g_4 + c_2\left(g_4^2/g_3\right) - c_3g_3 - c_4g_4$$
$$A_{44} = c_2(g_4/g_3) - c_4$$

As in the earlier case, because the system is only partially linearized, we are forced to evaluate the stability of the internal dynamics or the zero dynamics of the system. By setting $\phi_1 = \phi_2 = 0$, the equation for the zero dynamics is obtained as

$$\begin{Bmatrix} \dot{\phi}_3 \\ \dot{\phi}_4 \end{Bmatrix} = \begin{Bmatrix} A_{34}\phi_4 \\ [g_4Q_U(\phi_3) - g_3P_U(\phi_3)]\phi_3 + A_{44}\phi_4 \end{Bmatrix} \tag{23}$$

Unlike the preceding case, the zero dynamics is nonlinear and requires more careful analysis. At a first glance, the zero dynamics (23) has an equilibrium point $(\phi_3, \phi_4) = (0, 0)$. However, it turns out that, depending on the parameters U and a, additional equilibrium points exist, and we need to perform bifurcation analysis to completely understand the characteristics of the zero dynamics represented by Eq. (23). Two sets of bifurcation diagrams are shown in Figs. 6 and 7. Figure 6 shows the bifurcation diagram with respect to the flow velocity U and exhibits the so-called pitch-fork bifurcation.[28,29] In other words, up to a critical velocity U_{c1}, the zero dynamics has only one equilibrium point at (0, 0) and is stable. However, beyond U_{c1}, there exist two equilibrium points that are stable, whereas the original equilibrium point (origin) is unstable. If the velocity is greater than U_{c2}, all of the equilibrium points are unstable. We observe that the critical velocities U_{c_1} and U_{c_2} are dependent on the elastic axis location a and, generally, as the elastic axis is moved forward, the stable velocity region grows. A typical plot of stable and unstable manifolds is shown in Fig. 8. In this case there exist two stable equilibrium points and one unstable equilibrium point. A trajectory will be attracted to either one of the two stable equilibrium points depending on initial conditions. Figure 7 shows the bifurcation diagram with respect to the elastic axis location a. As one might expect, the stable region of a is smaller for the greater velocity.

With the initial conditions $y = 0.01$ m, $\alpha = 0.1$ rad, and $a = -0.68$ and $U = 15$ m/s, the time response of the controlled system is

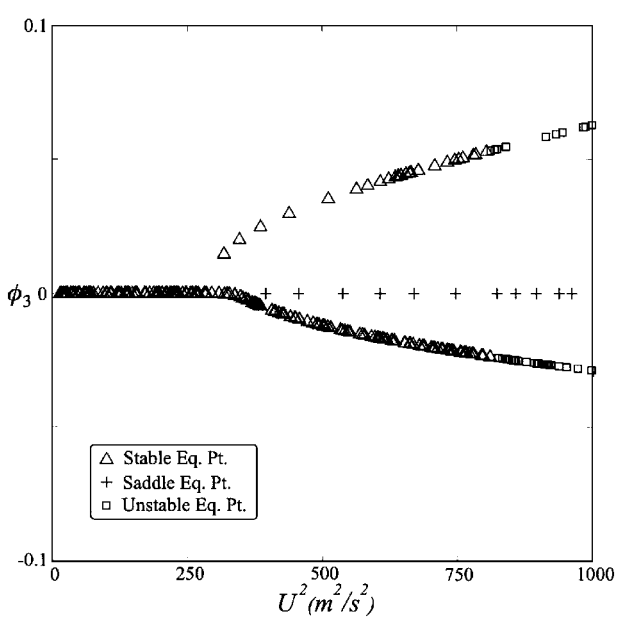

Fig. 6 Bifurcation diagram for zero dynamics for plunge primary control: $a = -0.63$ with respect to U^2.

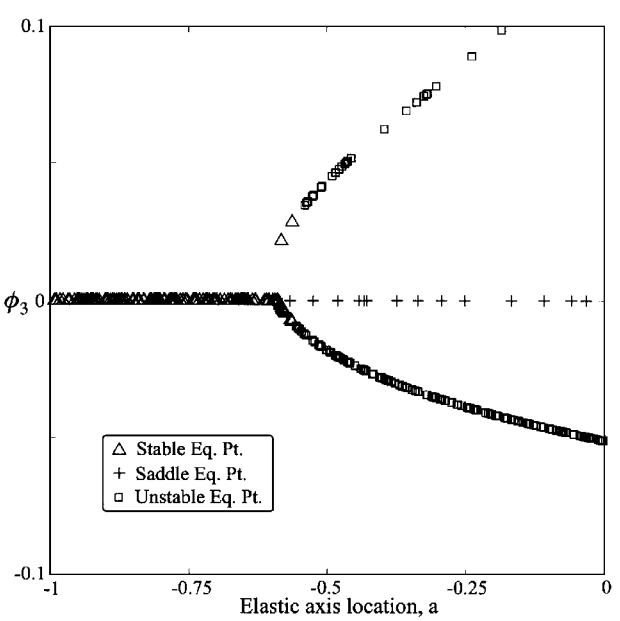

Fig. 7 Bifurcation diagram for zero dynamics for plunge primary control: $U^2 = 200$ m^2/s^2 with respect to a.

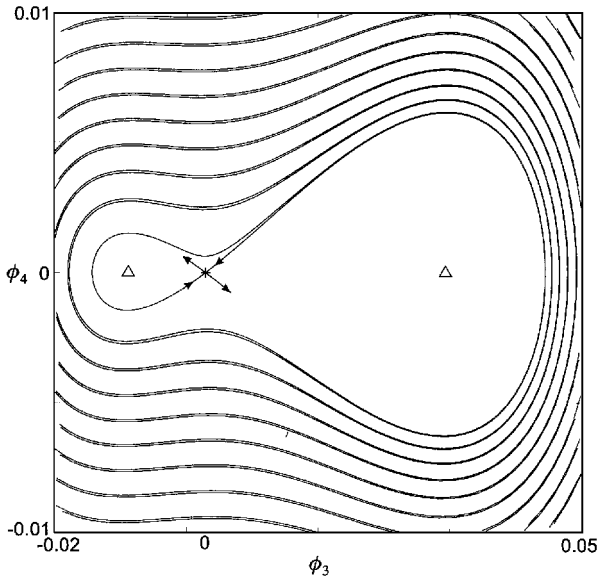

Fig. 8 Stable and unstable manifolds of equilibrium point (0, 0) for two stable and one unstable equilibrium case.

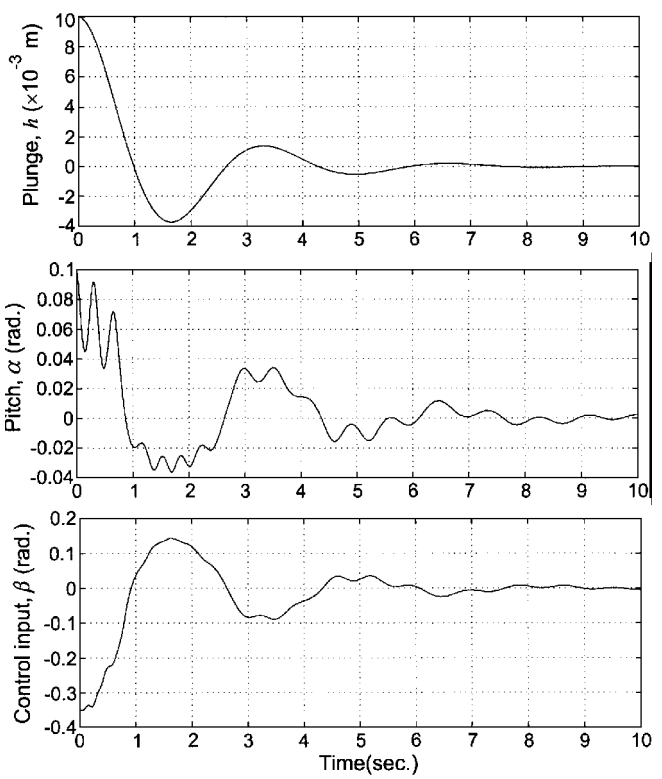

Fig. 9 Time response of plunge primary control: $a = -0.68$ and $U = 15$ m/s.

shown in Fig. 9. We have chosen the modified input $v = -1.2\dot{h} - 4h$ such that the closed subsystem has poles at $s = -0.6 \pm 1.9079$. As is expected, the plunge output h and $\dot{h}$ converges to zero.

V. Feedback Linearization with Two Control Surfaces

In the preceding two sections, we have shown that, by using a partial feedback linearization method, we can construct locally stable nonlinear controllers for the aeroelastic model. We obtained partially linearized systems and subsequently analyzed the zero dynamics to ensure the stability of the closed-loop system. However, because the system is only partially linearized, we were only able to obtain local stability results. In this section, we investigate the possibility of obtaining a globally stable nonlinear controller by adding an additional control surface.

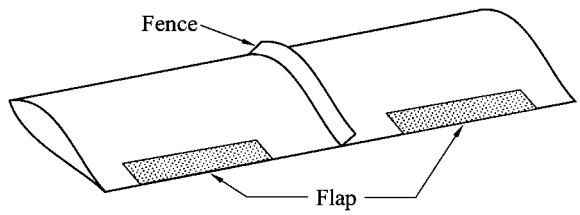

Fig. 10 Wing with two control surfaces.

By adding another control surface, we assume that the quasisteady lift and moment of the system is expressed as follows:

$$L = \rho U^2 b c_{l_\alpha}\left[\alpha + (\dot{h}/U) + \left(\tfrac{1}{2} - a\right)b(\dot{\alpha}/U)\right] + \rho U^2 b c_{l_{\beta_1}}\beta_1 + \rho U^2 b c_{l_{\beta_2}}\beta_2 \tag{24}$$

$$M = \rho U^2 b^2 c_{m_\alpha}\left[\alpha + (\dot{h}/U) + \left(\tfrac{1}{2} - a\right)b(\dot{\alpha}/U)\right] + \rho U^2 b^2 c_{m_{\beta_1}}\beta_1 + \rho U^2 b^2 c_{m_{\beta_2}}\beta_2 \tag{25}$$

The reader is advised that the assumption that the lift and moment can be expressed as simply as given in Eqs. (24) and (25) is very restrictive. In particular, it is only appropriate for wing sections that have a very large ratio of span to lateral separation of the control surfaces. As usual, it is likewise limited to small angle of attack and small control surface displacements. It can be a reasonable representation of lift and moment forces for low-speed flow in wind-tunnel models with the introduction of a fence or splitter plate as shown in Fig. 10.

Despite the limitations imposed by such a rudimentary aerodynamic model, there are compelling reasons for studying this system from a control theoretic standpoint. We show in this section that the system shown in Fig. 10 is exactly feedback linearizable provided we know the structural nonlinearities. As such, this analysis provides an approach for designing control systems in which we do not know the exact structure of nonlinearities.

To begin, we rewrite Eq. (2):

$$\begin{bmatrix} m & mx_\alpha b \\ mx_\alpha b & I_\alpha \end{bmatrix}\begin{Bmatrix} \ddot{h} \\ \ddot{\alpha} \end{Bmatrix} + \begin{bmatrix} c_h + \rho U b c_{l_\alpha} & \rho U b^2 c_{l_\alpha}\left(\frac{1}{2} - a\right) \\ \rho U b^2 c_{m_\alpha} & c_\alpha - \rho U b^3 c_{m_\alpha}\left(\frac{1}{2} - a\right) \end{bmatrix}\begin{Bmatrix} \dot{h} \\ \dot{\alpha} \end{Bmatrix} + \begin{bmatrix} k_h & \rho U^2 b c_{l_\alpha} \\ 0 & -\rho U^2 b^2 c_{m_\alpha} + k_\alpha(\alpha) \end{bmatrix}\begin{Bmatrix} h \\ \alpha \end{Bmatrix} = \begin{bmatrix} -\rho b c_{l_{\beta_1}} & -\rho b c_{l_{\beta_2}} \\ \rho b^2 c_{m_{\beta_1}} & \rho b^2 c_{m_{\beta_2}} \end{bmatrix}\begin{Bmatrix} \beta_1 \\ \beta_2 \end{Bmatrix} U^2 \tag{26}$$

In state-space form, Eq. (26) can be compactly written as

$$\dot{\boldsymbol{x}} = \boldsymbol{f}_\mu(\boldsymbol{x}) + \boldsymbol{g}_1(\boldsymbol{x})U^2\beta_1 + \boldsymbol{g}_2(\boldsymbol{x})U^2\beta_2 \tag{27}$$

where

$$\boldsymbol{f}_\mu = \begin{Bmatrix} x_3 \\ x_4 \\ -k_1 x_1 - [k_2 U^2 + p(x_2)]x_2 - c_1 x_3 - c_2 x_4 \\ -k_3 x_1 - [k_4 U^2 + q(x_2)]x_2 - c_3 x_3 - c_4 x_4 \end{Bmatrix}$$

$$\boldsymbol{g}_1 = \begin{Bmatrix} 0 \\ 0 \\ g_{13} \\ g_{14} \end{Bmatrix}, \qquad \boldsymbol{g}_2 = \begin{Bmatrix} 0 \\ 0 \\ g_{23} \\ g_{24} \end{Bmatrix}$$

Most of the variables in the preceding equation are defined in Table 1 except g_{ij}, which are defined as

$$g_{13} = (1/d)\left(-I_\alpha \rho b c_{l_{\beta_1}} - m x_\alpha b^3 \rho c_{m_{\beta_1}}\right)$$

$$g_{14} = (1/d)\left(m x_\alpha b^2 \rho c_{l_{\beta_1}} + m \rho b^2 c_{m_{\beta_1}}\right)$$

$$g_{23} = (1/d)\left(-I_\alpha \rho b c_{l_{\beta_2}} - m x_\alpha b^3 \rho c_{m_{\beta_2}}\right)$$

$$g_{24} = (1/d)\left(m x_\alpha b^2 \rho c_{l_{\beta_2}} + m \rho b^2 c_{m_{\beta_2}}\right)$$

Because we have two control surfaces, we consider two output functions such as

$$\boldsymbol{y}(\boldsymbol{x}) = \begin{Bmatrix} y_1(\boldsymbol{x}) \\ y_2(\boldsymbol{x}) \end{Bmatrix} = \begin{Bmatrix} x_1 \\ x_2 \end{Bmatrix} = \begin{Bmatrix} h \\ \alpha \end{Bmatrix} \tag{28}$$

To investigate the relative degree of this multiple-degree-of-freedom system, the following derivatives are needed. For the first output measurement,

$$y_1(\boldsymbol{x}) = x_1, \qquad L_{g_1} y_1(\boldsymbol{x}) = 0, \qquad L_{g_2} y_1(\boldsymbol{x}) = 0$$

$$L_f y_1(\boldsymbol{x}) = x_3, \qquad L_{g_1} L_f y_1(\boldsymbol{x}) = g_{13} \neq 0$$

$$L_{g_2} L_f y_1(\boldsymbol{x}) = g_{23} \neq 0$$

For the second output measurement, we require

$$y_2(\boldsymbol{x}) = x_2, \qquad L_{g_1} y_2(\boldsymbol{x}) = 0, \qquad L_{g_2} y_2(\boldsymbol{x}) = 0$$

$$L_f y_2(\boldsymbol{x}) = x_4, \qquad L_{g_1} L_f y_2(\boldsymbol{x}) = g_{14} \neq 0$$

$$L_{g_2} L_f y_2(\boldsymbol{x}) = g_{24} \neq 0$$

The following matrix plays a crucial role in defining a linearizing transformation, as will be shown shortly:

$$A(\boldsymbol{x}) = \begin{bmatrix} L_{g_1} L_f y_1(\boldsymbol{x}) & L_{g_2} L_f y_1(\boldsymbol{x}) \\ L_{g_1} L_f y_2(\boldsymbol{x}) & L_{g_2} L_f y_2(\boldsymbol{x}) \end{bmatrix} = \begin{bmatrix} g_{13} & g_{23} \\ g_{14} & g_{24} \end{bmatrix} \tag{29}$$

Substituting the definitions of g_{ij}, we have

$$A(\boldsymbol{x}) = \frac{1}{d}\begin{bmatrix} -I_\alpha \rho b c_{l_{\beta_1}} - m x_\alpha b^3 \rho c_{m_{\beta_1}} & -I_\alpha \rho b c_{l_{\beta_2}} - m x_\alpha b^3 \rho c_{m_{\beta_2}} \\ m x_\alpha b^2 \rho c_{l_{\beta_1}} + m \rho b^2 c_{m_{\beta_1}} & m x_\alpha b^2 \rho c_{l_{\beta_2}} + m \rho b^2 c_{m_{\beta_2}} \end{bmatrix} \tag{30}$$

The output functions have relative degree of $\{2, 2\}$ at $\boldsymbol{x}_0$ if the matrix $A(\boldsymbol{x})$ is nonsingular at $\boldsymbol{x}_0$. The determinant of the matrix $A(\boldsymbol{x})$ is calculated as

$$\begin{aligned} |A(\boldsymbol{x})| &= m^2 x_\alpha^2 b^5 \rho^2 \left(c_{l_{\beta_1}} c_{m_{\beta_2}} - c_{m_{\beta_1}} c_{l_{\beta_2}}\right) \\ &\quad + m I_\alpha \rho^2 b^3 \left(c_{m_{\beta_1}} c_{l_{\beta_2}} - c_{l_{\beta_1}} c_{m_{\beta_2}}\right) \\ &= m \rho^2 b^3 \left(m x_\alpha^2 b^2 - I_\alpha\right)\left(c_{l_{\beta_1}} c_{m_{\beta_2}} - c_{m_{\beta_1}} c_{l_{\beta_2}}\right) \end{aligned}$$

Thus, unless $m x_\alpha^2 b^2 = I_\alpha$, the nonsingularity of the control influence matrix guarantees that the system is completely feedback linearizable. Note that this result agrees with our intuition. Suppose, for example, that $c_{l_{\beta_1}} = c_{l_{\beta_2}}$. In this case, the control influence matrix is not invertible, and the preceding results do not hold. In fact, the wing section control system is equivalent to a single control surface system in this case. Assuming that $A(\boldsymbol{x})$ is nonsingular, define the state transformation as

$$\begin{aligned} \phi_1 &= y_1 = x_1 (= h), & \phi_2 &= L_f y_1 = x_3 (= \dot{h}) \\ \phi_3 &= y_2 = x_2 (= \alpha), & \phi_2 &= L_f y_2 = x_4 (= \dot{\alpha}) \end{aligned} \tag{31}$$

The transformed equation of motion is then

$$\begin{aligned} \dot{\phi}_1 &= \phi_2, & \dot{\phi}_2 &= L_f^2 y_1 + L_{g_1} L_f y_1 U^2 \beta_1 + L_{g_2} L_f y_1 U^2 \beta_2 \\ \dot{\phi}_3 &= \phi_4, & \dot{\phi}_4 &= L_f^2 y_1 + L_{g_1} L_f y_2 U^2 \beta_1 + L_{g_2} L_f h_2 U^2 \beta_2 \end{aligned} \tag{32}$$

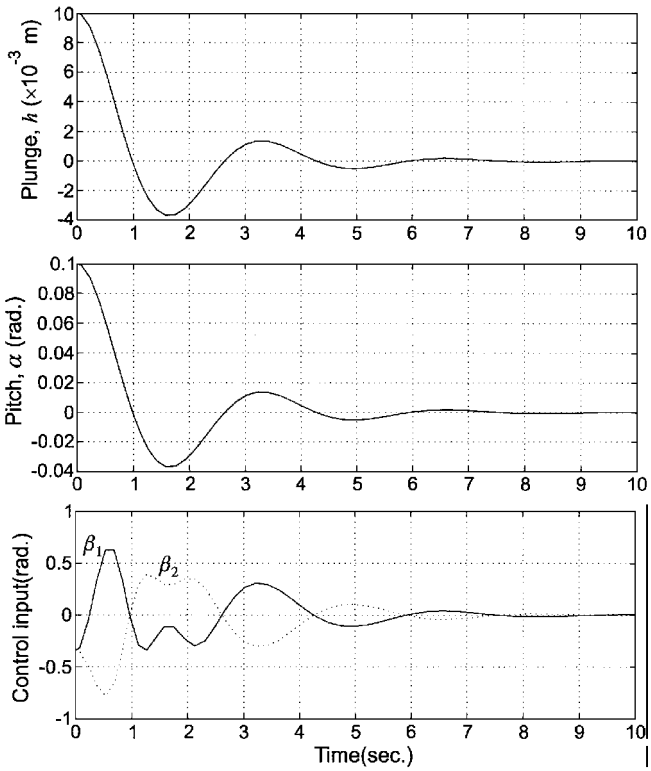

Fig. 11 Time response with two control surfaces: $a = -0.4$ and $U = 15$ m/s.

Observe that

$$\begin{Bmatrix} \dot{\phi}_2 \\ \dot{\phi}_4 \end{Bmatrix} = \begin{Bmatrix} L_f^2 h_1 \\ L_f^2 h_1 \end{Bmatrix} + \begin{bmatrix} L_{g_1} L_f y_1(\boldsymbol{x}) & L_{g_2} L_f y_1(\boldsymbol{x}) \\ L_{g_1} L_f y_2(\boldsymbol{x}) & L_{g_2} L_f y_2(\boldsymbol{x}) \end{bmatrix} \begin{Bmatrix} \beta_1 \\ \beta_2 \end{Bmatrix}$$

$$= \boldsymbol{b}(\boldsymbol{x}) + A(\boldsymbol{x}) U^2 \boldsymbol{\beta}$$

By choosing

$$\boldsymbol{\beta} = -U^{-2} A^{-1}(\boldsymbol{x})(\boldsymbol{b} + \boldsymbol{v}) \tag{33}$$

we obtain the completely feedback linearized system

$$\dot{\phi}_1 = \phi_2, \qquad \dot{\phi}_2 = v_1, \qquad \dot{\phi}_3 = \phi_4, \qquad \dot{\phi}_4 = v_2 \tag{34}$$

With the same initial conditions as before, i.e., $a = -0.4$, $U = 15$ m/s, $\alpha = 0.1$ rad, and $y = 0.01$ m, the time response of the controlled system is shown in Fig. 11. The fictitious input

$$\boldsymbol{v} = \begin{Bmatrix} -1.2\dot{h} - 4h \\ -1.2\dot{\alpha} - 4\alpha \end{Bmatrix}$$

is selected such that the closed linearized system has eigenvalues at $\lambda = \{-0.6 \pm 1.9079, -0.6 \pm 1.9079\}$.

VI. Conclusion

We have applied a feedback linearization methodology to design nonlinear controllers for a typical wing section with structural nonlinearities. Without any control effort, or with linear controllers, the aeroelastic system reveals various kinds of nonlinear phenomena including LCOs as noted in various texts. The nonlinear controllers based on the partial feedback linearization yielded a stable closed-loop system, although the stability is guaranteed in the neighborhood of the equilibrium points. The two crucial parameters, elastic axis location and freestream velocity, each have a significant effect on the resulting partially linearized closed-loop system. To derive a globally stabilizing controller, a controller based on two control surfaces has been derived. Under the assumption that the two control surfaces are independent, the nonlinear controller showed exceptional performance in stabilizing the aeroelastic system.

References

[1]Fung, Y. C., *An Introduction to the Theory of Aeroelasticity*, Wiley, New York, 1955, pp. 207–215.

[2]Theodorsen, T., "General Theory of Aerodynamic Instability and the Mechanism of Flutter," NACA Rept. 496, 1935.

[3]Theodorsen, T., and Garrick, I. E., "Mechanism of Flutter: A Theoretical and Experimental Investigation of the Flutter Problem," NACA Rept. 685, 1940.

[4]Lyons, M. G., Vepa, R., McIntosh, I. E., and DeBra, D. B., "Control Law Synthesis and Sensor Design for Active Flutter Suppression," *Proceedings of the AIAA Guidance and Control Conference*, AIAA, New York, 1973, pp. 1–29 (AIAA Paper 73-832).

[5]Vepa, R., "On the Use of Padé Approximants to Represent Unsteady Aerodynamic Loads for Arbitrary Small Motions of Wings," AIAA Paper 76-17, 1976.

[6]Edwards, J. W., Ashley, H., and Breakwell, J., "Unsteady Aerodynamic Modeling for Arbitrary Motions," *AIAA Journal*, Vol. 17, No. 4, 1979, pp. 365–374.

[7]Mukhopadhyay, V., Newsom, J. R., and Abel, I., "A Direct Method for Synthesizing Low-Order Optimal Feedback Control Laws with Application to Flutter Suppression," *Proceedings of the Atmospheric Flight Mechanics Conference*, AIAA, New York, 1980, pp. 465–475 (AIAA Paper 80-1613).

[8]Gangsaas, D., Ly, U., and Norman, D. C., "Practical Gust Load Alleviation and Flutter Suppression Control Laws Based on LQG Methodology," AIAA Paper 81-0021, Jan. 1981.

[9]Karpel, M., "Design for Active Flutter Suppression and Gust Alleviation Using State-Space Aeroelastic Modeling," *Journal of Aircraft*, Vol. 19, No. 3, 1982, pp. 221–227.

[10]Horikawa, H., and Dowell, E. H., "An Elementary Explanation of the Flutter Mechanism with Active Feedback Controls," *Journal of Aircraft*, Vol. 16, No. 4, 1979, pp. 225–232.

[11]Heeg, J., "Analytical and Experimental Investigation of Flutter Suppression by Piezoelectric Actuation," NASA TP 3241, 1993.

[12]Lin, C. Y., "Strain Actuated Aeroelastic Control," M.S. Thesis, Dept. of Aeronautics and Astronautics, Massachusetts Inst. of Technology, Cambridge, MA, Feb. 1993.

[13]Lazarus, K., "Multivariable High-Authority Control of Plate-Like Active Lifting Surfaces," Ph.D. Dissertation, Dept. of Aeronautics and Astronautics, Massachusetts Inst. of Technology, Cambridge, MA, June 1992.

[14]Lazarus, K., Crawley, E., and Lin, C., "Fundamental Mechanisms of Aeroelastic Control with Control Surface and Strain Actuation," *Journal of Guidance, Control, and Dynamics*, Vol. 18, No. 1, 1995, pp. 10–17.

[15]Woolston, D. S., Runyan, H. L., and Andrews, R. E., "An Investigation of Effects of Certain Types of Structural Nonlinearities on Wing and Control Surface Flutter," *Journal of the Aeronautical Sciences*, Vol. 24, No. 1, 1957, pp. 57–63.

[16]Breitbach, E. J., "Effects of Structural Nonlinearities on Aircraft Vibration and Flutter," AGARD-R-665, Jan. 1978.

[17]Tang, D. M., and Dowell, E. H., "Flutter and Stall Response of a Helicopter Blade with Structural Nonlinearity," *Journal of Aircraft*, Vol. 29, No. 5, 1990, pp. 953–960.

[18]Lee, B. H. K., and LeBlanc, P., "Flutter Analysis of a Two-Dimensional Airfoil with Cubic Nonlinear Restoring Force," National Aeronautical Establishment, Aeronautical Note 36, Canada National Research Council No. 25438, Ottawa, PQ, Canada, Feb. 1986.

[19]O'Neil, T., and Strganac, T. W., "An Experimental Investigation of Nonlinear Aeroelastic Response," *Journal of Aircraft* (to be published).

[20]O'Neil, T., and Strganac, T. W., "Nonlinear Aeroelastic Response—Analyses and Experiments," AIAA Paper 96-0014, Jan. 1996.

[21]O'Neil, T., Gilliatt, H. C., and Strganac, T. W., "Investigations of Aeroelastic Response for a System with Continuous Structural Nonlinearities," AIAA Paper 96-1390, April 1996.

[22]Block, J. J., and Strganac, T. W., "Applied Active Control for a Nonlinear Aeroelastic Structure," *Journal of Guidance, Control, and Dynamics* (submitted for publication).

[23]Dowell, E. H., "Nonlinear Aeroelasticity," *Proceedings of the AIAA 31st Structures, Structural Dynamics, and Materials Conference*, AIAA, Washington, DC, 1990, pp. 1497–1509.

[24]Yang, Z. C., and Zhao, L. C., "Analysis of Limit Cycle Flutter of an Airfoil in Incompressible Flow," *Journal of Sound and Vibration*, Vol. 123, No. 1, 1988, pp. 1–13.

[25]Zhao, L. C., and Yang, Z. C., "Chaotic Motions of an Airfoil with Nonlinear Stiffness in Incompressible Flow," *Journal of Sound and Vibration*, Vol. 138, No. 2, 1990, pp. 245–254.

[26]Isidori, A., *Nonlinear Control Systems*, Springer–Verlag, New York, 1989, pp. 1–82.

[27]Slotine, J. E., and Li, W., *Applied Nonlinear Control*, Prentice–Hall, Englewood Cliffs, NJ, 1991, pp. 207–275.

[28]Guckenheimer, J., and Holmes, P., *Nonlinear Oscillations, Dynamical Systems, and Bifurcations of Vector Fields*, Springer–Verlag, New York, 1983, pp. 117–165.

[29]Wiggins, S., *Introduction to Applied Nonlinear Dynamical Systems, and Chaos*, Springer–Verlag, New York, 1990, pp. 253–419.